ISSN 0021-3640, JETP Letters, 2021, Vol. 114, No. 9, pp. 556–560. © The Author(s), 2021. This article is an open access publication.

CONDENSED MATTER

Cu-Site Disorder in $CuAl_2O_4$ as Studied by XPS Spectroscopy

I. S. Zhidkov[a, b, *], A. A. Belik[c], A. I. Kukharenko[a], S. O. Cholakh[a], L. S. Taran[b], A. Fujimori[d], S. V. Streltsov[a, b], and E. Z. Kurmaev[a, b]

[a] *Institute of Physics and Technology, Ural Federal University, Yekaterinburg, 620002 Russia*

[b] *Mikheev Institute of Metal Physics, Ural Branch, Russian Academy of Sciences, Yekaterinburg, 620108 Russia*

[c] *International Center for Materials Nanoarchitectonics (WPI-MANA), National Institute for Materials Science (NIMS), Tsukuba, Ibaraki, 305-0044 Japan*

[d] *Department of Applied Physics, Waseda University, Shinjuku-ku, Tokyo, 169-8555 Japan*

**e-mail: i.s.zhidkov@urfu.ru*

Received September 21, 2021; revised September 30, 2021; accepted September 30, 2021

The results of full study of X-ray photoelectron spectra (XPS) of spin-liquid candidate $CuAl_2O_4$ including the measurements of high-energy resolved core level (Cu $2p$, Al $3p$, O $1s$), Cu LMM Auger and valence band spectra are presented. The comparison of obtained results with spectra of reference samples and specially performed density functional theory calculations has confirmed a finite Cu site-disorder in $CuAl_2O_4$, where about 30% of Cu^{2+} ions occupy the octahedral sites. Obtained valence band spectra can be used in further theoretical studies aimed on the investigation of electronic and magnetic properties of this mysterious material.

DOI: 10.1134/S0021364021210062

1. INTRODUCTION

The AB_2O_4 oxides with spinel structure are one of the most interesting classes of modern ceramic materials due to their physical and chemical properties that determine their technological application. For example, copper aluminate ($CuAl_2O_4$) is used as a gas sensor [1], a catalyst in the oxidation of benzyl alcohol [2], steam reforming of methanol [3], a photocatalyst for the decomposition of pollutants in an aqueous solution [4], a solar energy absorber [5] solar water-splitting [6], etc. Therefore, for the development of these technologies, so much attention is paid to theoretical and experimental studies of various spinels and, first of all, to the study of fundamental properties that are determined primarily by its crystal structure. In $CuAl_2O_4$ spinel the Cu^{2+}-ions must be located in the center of A-tetrahedral sites and non-magnetic Al^{3+} ions are in the center of octahedral B-sites. In this case, the Cu^{2+} d-states split into t_2 and e states. The degeneracy of t_{2g}-states can be removed through the following two channels: due to spin–orbit coupling and Jahn–Teller distortion, which lowers the T_d symmetry of the crystal field. As a rule, the results of X-ray and neutron diffraction studies show that the crystal structure of $CuAl_2O_4$ at atmospheric pressure is cubic without any signs of tetragonal distortion [4].

However, possible stabilization of the cubic phase (contradicting to the Jahn–Teller theorem) inevitable leads to formation of the spin–orbit entangled $J_{\text{eff}} = 1/2$ state and strong exchange anisotropy, which may result in the spin-liquid ground state [7, 8]. This hypothesis was used in particular to explain absence of the long-range magnetic order in $CuAl_2O_4$ even at very low temperature [8]. Alternative explanation is based on presence of intrinsic disorder between tetra and octa sites, which prevents onset of antiferromagnetism.

It is no coincidence that in some early works it was assumed that about 30% of Cu^{2+} ions occupy octahedral positions [4, 5]. In this connection, of particular interest is the use of local spectral methods sensitive to the nearest surrounding of the exciting atoms. In connection with this in recent years, the resonant inelastic X-ray scattering (RIXS) has been used for this purpose [9]. In this work, we applied another method of X-ray photoelectron spectroscopy, which is also an element- and a site-selective probe.

2. EXPERIMENTAL AND CALCULATION DETAILS

$CuAl_2O_4$ was prepared from a stoichiometric mixture of Al_2O_3 (99.9%) and CuO (99.9%). The mixture was pressed into a pellet and annealed on Pt foil at 1193 K for 84 h and at 1293 K for 38 h in air with several intermediate grindings. This phase will be called ambient-pressure $CuAl_2O_4$, and it had orange–brown

color. X-ray powder diffraction (XRPD) data were collected at room temperature on a RIGAKU Mini-Flex 600 diffractometer using Cu $K\alpha$ radiation (2 range of 8°–140°, a step width of 0.02°, and a scan rate of 1°/min). XRPD data were analyzed by the Rietveld method using RIETAN-2000 [10]. $CuAl_2O_4$ prepared at ambient pressure was single phase and had sharp reflections on XRPD patterns. The structural analysis gave the following cation distribution $[Cu_{0.676}Al_{0.324}]_{8a}[Al_{1.676}Cu_{0.324}]_{16d}O_4$. The similar distribution was found in the literature for samples prepared at ambient pressure (for example, $[Cu_{0.68}Al_{0.32}]_{8a}[Al_{1.68}Cu_{0.32}]_{16d}O_4$ in [8] or $x = 0.36$–0.39 for $[Cu_{1-x}Al_x]_{8a}[Al_{2-x}Cu_x]_{16d}O_4$ in [11]).

X-ray photoelectron spectroscopy (XPS) was used to measure core excitation with help of a PHI XPS 5000 VersaProbe spectrometer (ULVAC-Physical Electronics, USA) with a spherical quartz monochromator and an energy analyzer working in the range of binding energies from 0 to 1500 eV. The X-ray spot size was 200 μm and Al $K\alpha$ radiation (1486 eV) was used. The energy resolution was $\Delta E \le 0.5$ eV. The samples were measured at a pressure below 10^{-7} Pa. All spectra were calibrated using C 1*s* binding energies of adventitious carbon (285 eV). Finally, all spectra were processed using PHI MultiPak 9.9.0.8 software.

The calculations of $CuAl_2O_4$ and $Cu(OH)_2$ compounds were carried out using the Vienna ab initio simulation package [12], which was previously used to study such transition metal compounds as, e.g., $Ba_4NbMn_3O_{12}$ [13] or ZrC_{l3} [14]. We utilized the projector augmented-wave method with the Perdew–Burke–Ernzerhof type of exchange correlation functional [15] within the general gradient approximation (GGA + *U*) [16]. Initial crystal structure parameters were taken for $CuAl_2O_4$ from [6] ($T = 40$ K). On-site Coulomb repulsion parameter *U* was taken to be 7 eV, while Hund's intra-atomic exchange is $J_H = 1$ eV. The spin–orbit coupling was taken into account in the calculations.

3. RESULTS AND DISCUSSION

Figure 1 shows the XPS survey spectra of samples under study. The numerical values of the surface composition (in at %) obtained from these spectra are given in Table 1. Note that the ratio of the concentrations of the atoms of the components as a whole follows the chemical formula of the compound and the level of carbon contamination is quite low.

Figure 2a displays (a) XPS Cu 2*p* and (b) Auger Cu LMM spectra of $CuAl_2O_4$. The XPS Cu $2p_{3/2}$ spectrum has two peak structure (Cu_1 and Cu_2) and is shifted to high-energy side (towards CuO) with respect to that of Cu and Cu_2O. Another feature of bivalent copper in $CuAl_2O_4$ is the presence of a CT (charge transfer) satellite S at the same binding energy as in

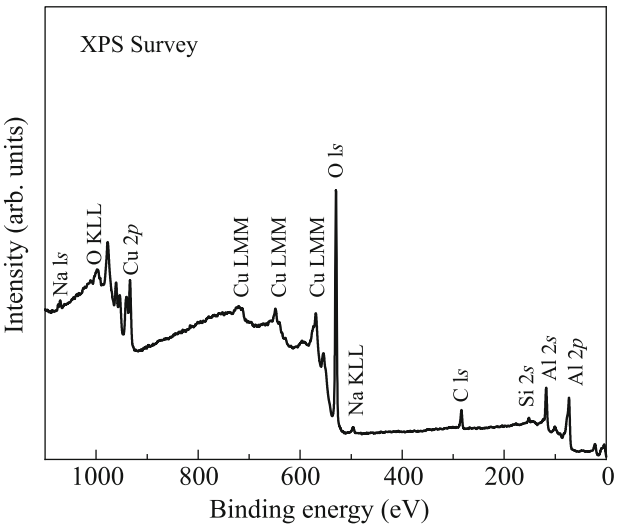

Fig. 1. XPS Survey spectra.

CuO arising from multiplet splitting effects due to the interaction between the Cu 2*p* core hole and the $3d^9$ electronic configuration [17]. The Auger Cu LMM spectra (Fig. 2b) also provide the evidence that the main oxidation state of copper in $CuAl_2O_4$ is 2+ [18].

The spectra shown in Fig. 3 make it possible to determine the charge state of aluminum and oxygen atoms in the compound under consideration. As follows from the analysis of these spectra, the XPS Al 2*p* spectrum coincides in energy position with that in Al_2O_3, which means that Al atoms are trivalent. XPS O 1*s* spectrum shows that the contribution of hydroxyl groups [19] is noticeably much smaller than that from the lattice oxygen in $CuAl_2O_4$.

Let us consider the origin of the two-peak structure (Cu_1 and Cu_2) of the XPS Cu 2*p* spectrum of $CuAl_2O_4$ shown in Fig. 2a. It is generally believed that $CuAl_2O_4$ at atmospheric pressure is in the cubic phase without any signs of tetragonal distortion [8]. This is the spin–orbit coupling, which can be responsible for suppression of the Jahn–Teller distortions and absence of corresponding splitting in the Cu-t_2 states [20]. However, the local symmetry breaking in this compound induced by Jahn–Teller distortions cannot be completely ruled out, since for this the spin–orbit coupling constant must exceed some critical value $\lambda_C \sim 0.3g^2/2B$, where *g* is the vibronic coupling parameter and *B* is the stiffness constant [21].

Table 1. Surface composition of $CuAl_2O_4$ (in at %)

Sample	C	O	Cu	Al	Na	Si	K
$CuAl_2O_4$	9	53.8	11.1	22.2	1.4	2.3	0.2

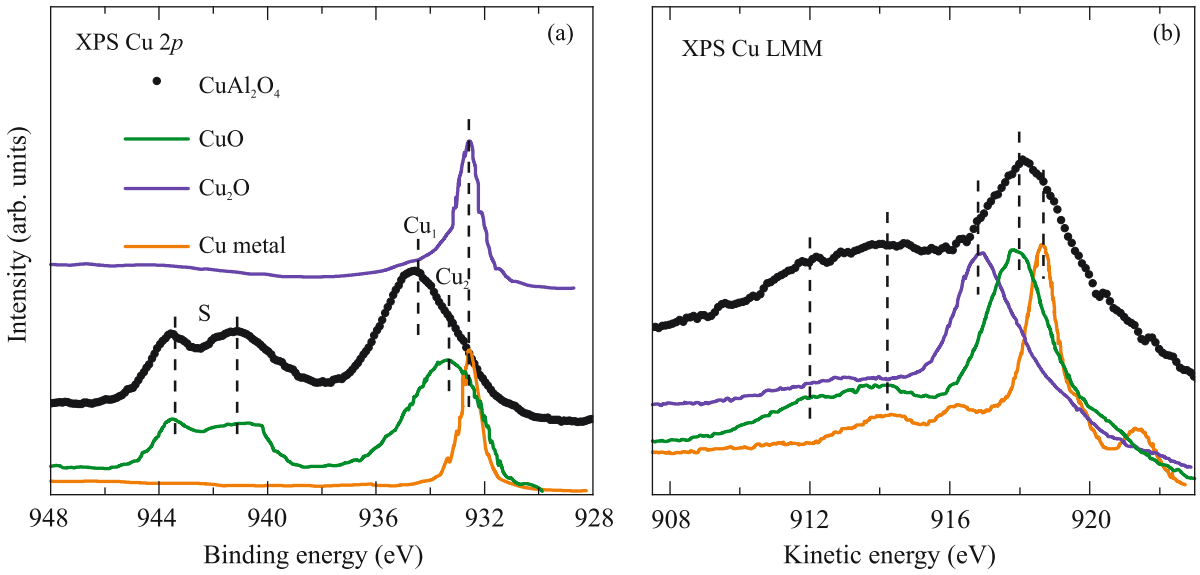

Fig. 2. (Color online) (a) XPS Cu 2*p* and (b) Auger Cu LMM spectra of $CuAl_2O_4$. The reference spectra are taken from [17, 18].

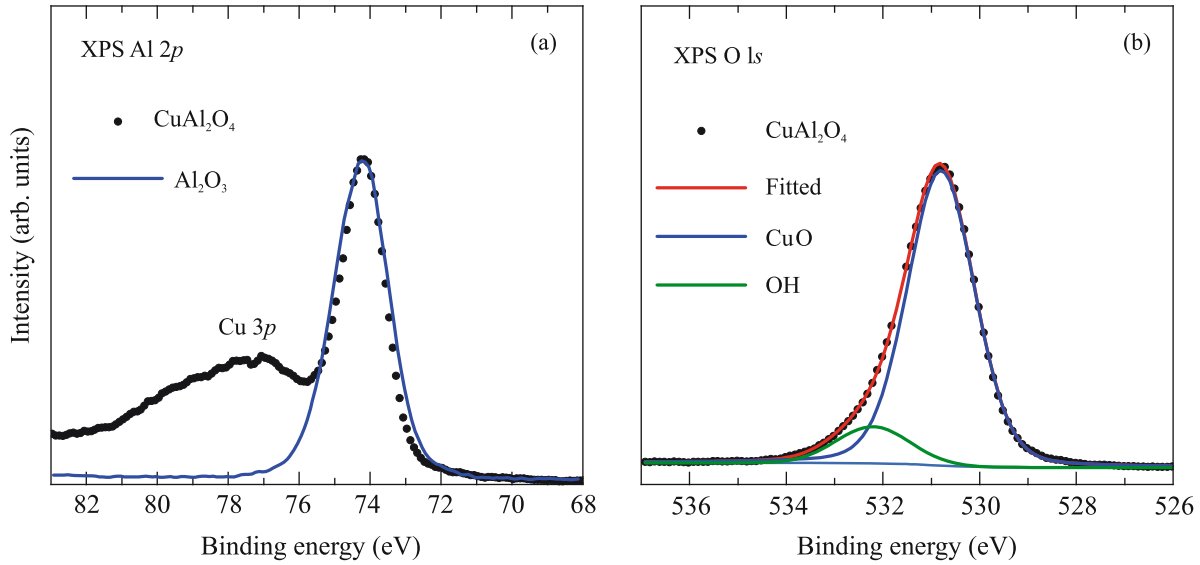

Fig. 3. (Color online) XPS Al 2*p* and O 1*s* of $CuAl_2O_4$.

The energy difference of Cu_1 and Cu_2 peaks in XPS Cu 2*p* spectra of $CuAl_2O_4$ is found around 1.2 eV (see Fig. 2a), which is much larger than possible splitting due to both the spin–orbit coupling or the crystal-field splitting because of the Jahn–Teller distortions. In fact, this energy difference is comparable with value fixed in splitting of Cu *L* XAS spectra [9] and the ratio of their intensities suggests that the Cu_1 and Cu_2 peaks correspond to the contributions of tetra- and octa-sites, respectively, and estimates degree of disorder in 30%. Therefore, we can conclude that the independent site-selective and element-selective X-ray measurements confirm a finite site-disorder in $CuAl_2O_4$.

The results of the total density of electronic states calculations of $CuAl_2O_4$ performed in DFT + *U* approach and taken into account spin–orbit coupling (Total DOS SOC) and Jahn–Teller distortion (Total DOS J_{eff}) are presented in Fig. 4. The comparison of the obtained results shows that taking into account the spin–orbit coupling does not lead to significant changes in the distribution of the total density of occupied states. The energy separation of the main peaks of the calculated total density of states is well reproduced

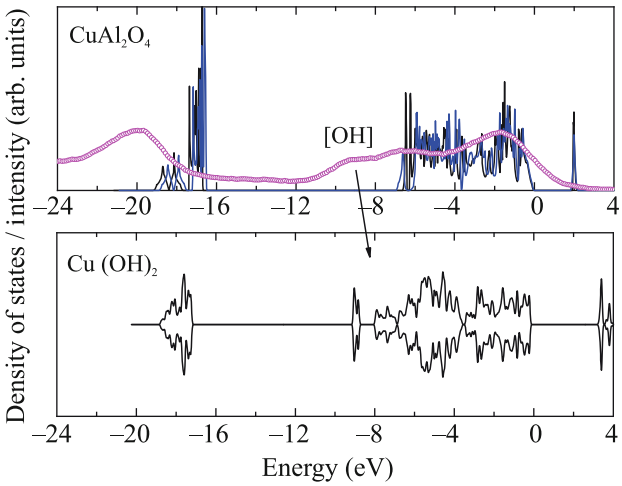

Fig. 4. (Color online) XPS valence band of $CuAl_2O_4$ results of DFT + U + SOC calculations of $CuAl_2O_4$. Two different solutions based on the spin–orbit entangled $J_{eff} = 1/2$ state and Jahn–Teller stabilized $S = 1/2$ states are used. The black line is the total DOS(J_{eff}), the blue line is the total DOS (SOC), and magenta circles demonstrate the XPS valence band spectrum of $CuAl_2O_4$.

by the XPS valence band spectrum also shown in this figure except the presence of an additional feature in the energy range of 8–10 eV. Earlier, a similar feature was recorded in the XPS valence band spectra of other transition metal compounds and was attributed to contribution of $(OH)^-$ hydroxyl group [22]. To check the origin of this feature in our case, we carried out an additional DFT calculation of the $Cu(OH)_2$ compound, which actually showed the presence of an additional band in this energy range. This is consistent also with the results of measurements of the XPS O 1*s* spectra shown in Fig. 3b where the contribution of the hydroxyl group is also recorded.

In conclusion, we studied electronic properties of $CuAl_2O_4$, which is actively investigated now because of possible realization of the spin-liquid state [8], suppression of long-range magnetic ordering and Jahn–Teller distortions due to the spin–orbital entanglement [7, 20]. Our results show the presence of a substantial Cu–Al disorder by the XPS measurements. This disorder may affect formation of an antiferromagnetic order and development of static Jahn–Teller distortions.

FUNDING

The DFT calculations were supported by the Russian Science Foundation (project no. 20-62-46047). The XPS measurements were supported by the Ministry of Science and Higher Education of the Russian Federation (theme Electron no. AAAA-A18-118020190098-5 and project FEUZ 2020-0060). I.S. Zhidkov acknowledges the support of the Council of the President of the Russian Federation for State Support of Young Scientists and Leading Scientific Schools (project no. MK-989.2020.2).

CONFLICT OF INTEREST

The authors declare that they have no conflicts of interest.

OPEN ACCESS

REFERENCES

1. J. J. Vijaya, L. J. Kennedy, G. Sekaran, M. Bayhan, and M. A. William, Sens. Actuators B **134**, 604 (2008).
2. C. Ragupathi, J. J. Vijaya, L. J. Kennedy, and M. Bououdina, Mater. Sci. Semicond. Process. **24**, 146 (2014).
3. Y. H. Huang, S. F. Wang, A. P. Tsai, and S. Kameoka, Ceram. Int. **40**, 4541 (2014).
4. W. Lv, B. Liu, Q. Qiu, F. Wang, Z. Luo, P. Zhang, and S. Wei, J. Alloys Compd. **479**, 480 (2009).
5. D. Ding, W. Cai, M. Long, H. Wu, and Y. Wu, Sol. Energy Mater. Sol. Cells **94**, 1578 (2010).
6. R. Tan, S. W. Hwang, A. Sivanantham, and I. S. Cho, J. Catal. **400**, 218 (2021).
7. S. A. Nikolaev, I. V. Solovyev, A. N. Ignatenko, V. Y. Irkhin, and S. V. Streltsov, Phys. Rev. B **98**, 201106 (2018).
8. R. Nirmala, K.-H. Jang, H. Sim, H. Cho, J. Lee, N.-G. Yang, S. Lee, R. M. Ibberson, K. Kakurai, M. Matsuda, S.-W. Cheong, V. V. Gapontsev, S. V. Streltsov, and J.-G. Park, J. Phys.: Condens. Matter. **29**, 13LT01 (2017).
9. H. Cho, C. H. Kim, Y. Lee, K. Komatsu, B. G. Cho, D. Y. Cho, T. Kim, C. Kim, Y. Kim, T. Y. Koo, Y. Noda, H. Kagi, D. I. Khomskii, D. Seoung, and J. G. Park, Phys. Rev. B **103**, L081101 (2021).
10. F. Izumi and T. Ikeda, Mater. Sci. Forum **321**, 198 (2000).
11. H. O'Neill, M. James, W. A. Dollase, and S. A. T. Redfern, Eur. J. Miner. **17**, 581 (2005).
12. G. Kresse and J. Hafner, Phys. Rev. B **47**, 558 (1993).

13. S. V. Streltsov and D. I. Khomskii, JETP Lett. **108**, 686 (2018).
14. A. V. Ushakov, I. V. Solovyev, and S. V. Streltsov, JETP Lett. **112**, 686 (2020).
15. J. P. Perdew, K. Burke, and M. Ernzerhof, Phys. Rev. Lett. **77**, 3865 (1996).
16. A. I. Liechtenstein, V. I. Anisimov, and J. Zaanen, Phys. Rev. B **52**, R5467 (1995).
17. M. C. Biesinger, Surf. Interface Anal. **49**, 1325 (2017).
18. M. C. Biesinger, L. W. M. Lau, A. R. Gerson, and R. S. C. Smart, Appl. Surf. Sci. **257**, 887 (2010).
19. S. Yamamoto, H. Bluhm, K. Anderson, G. Ketteler, H. Ogasawara, M. Salmeron, and A. Nilsson, J. Phys.: Condens. Matter **20**, 184025 (2008).
20. C. H. Kim, S. Baidya, H. Cho, V. V. Gapontsev, S. V. Streltsov, D. I. Khomskii, J.-G. Park, A. Go, and H. Jin, Phys. Rev. B **100**, 161104 (2019).
21. S. V. Streltsov and D. I. Khomskii, Phys. Rev. X **10**, 031043 (2020).
22. M. Fusi, E. Maccallini, T. Caruso, C. S. Casaria, A. li Bassi, C. E. Bottani, P. Rudolf, K. C. Prince, and R. G. Agostino, Surf. Sci. **605**, 333 (2011).